

# Dark Energy Models in the $w - w'$ Plane

Robert J. Scherrer

*Department of Physics and Astronomy, Vanderbilt University, Nashville, TN 37235*

We examine the behavior of dark energy models in the plane defined by  $w$  (the equation of state parameter for the dark energy) and  $w'$  (the derivative of  $w$  with respect to the logarithm of the scale factor). For non-phantom barotropic fluids with positive squared sound speed, we find that  $w' < 3w(w + 1)$ , the opposite of the bound on quintessence models previously derived by Caldwell and Linder. Thus, these barotropic models and quintessence models for the dark energy occupy disjoint regions in the  $w - w'$  plane. We also derive two new bounds for quintessence models in the  $w - w'$  plane: the first is a general bound for any scalar field with a monotonic potential, while the second improves on the Caldwell-Linder bound for tracker quintessence models. Observationally distinguishing barotropic models from quintessence models requires  $\sigma(w') \lesssim 1 + w$ .

## I. INTRODUCTION

Observations indicate that roughly 70% of the total energy density in the universe is in the form of dark energy, which has negative pressure and drives the late-time acceleration of the universe (see Ref. [1] for a recent review, and references therein).

The simplest model for this dark energy is a cosmological constant, but many other alternatives have been put forward. One possibility, dubbed quintessence, is a model in which the dark energy arises from a scalar field [2, 3, 4, 5, 6]. In another class of models, the dark energy is simply taken to be barotropic fluid, in which the pressure  $p$  and energy density  $\rho$  are related by

$$p = f(\rho). \quad (1)$$

The prototype for this sort of model is the Chaplygin gas [7, 8], which can be considered a special case of the generalized Chaplygin gas [9]. Although originally proposed as unified models for dark matter and dark energy, the Chaplygin gas and generalized Chaplygin gas models have also been examined as models for dark energy alone [10, 11, 12, 13, 14]. Interest in barotropic fluids as dark energy has not been confined to the generalized Chaplygin gas. Many other models have been proposed, including, e.g., the Van der Waals model [15] and the wet dark fluid model [16].

Obviously, it is important to determine whether these models can be distinguished by their observational consequences. In this vein, Caldwell and Linder [17] examined the behavior of quintessence models in the plane defined by the quantities  $w$  and  $w'$  for the dark energy. Here  $w$  is the ratio of pressure to density for the dark energy:

$$w = p/\rho, \quad (2)$$

and  $w'$  is the derivative of  $w$  with respect to the logarithm of the scale factor  $a$ :

$$w' = \frac{dw}{d\ln(a)}. \quad (3)$$

Caldwell and Linder showed that quintessence models in which the scalar field potential asymptotically ap-

proaches zero can be divided naturally into two categories, which they dubbed “freezing” and “thawing” models, with quite different behavior in the  $w - w'$  plane.

Here we extend and generalize these results. In the next section, we determine the behavior of general non-phantom barotropic fluids with positive squared sound speed in the  $w - w'$  plane, and we show that these models occupy a region of phase space which is disjoint from that occupied by quintessence models. In Section 3, we re-examine the lower bound on  $w'$  from Ref. [17]; we derive a new bound for a more general class of quintessence models, and sharpen the bound from Ref. [17] for the case of tracker potentials. These results are discussed in Section 4. Our results support the argument that the behavior of dark energy models in the  $w - w'$  plane provides a useful discriminator for such models.

## II. BAROTROPIC FLUIDS

As noted in the previous section, a barotropic fluid is one for which the pressure is purely a function of the density,  $p = f(\rho)$ . For such models, we have

$$w' = \frac{dw}{d\rho} \frac{d\rho}{d\ln(a)}. \quad (4)$$

The factors in this equation are given by

$$\frac{dw}{d\rho} = \frac{1}{\rho} \left( \frac{dp}{d\rho} - w \right), \quad (5)$$

and

$$\frac{d\rho}{d\ln(a)} = -3(1 + w)\rho. \quad (6)$$

Then the expression for  $w'$  becomes

$$w' = -3(1 + w) \left( \frac{dp}{d\rho} - w \right). \quad (7)$$

In order to derive useful constraints from equation (7), we need to assume something about the behavior of  $dp/d\rho$  and  $w$ . We will assume first that we are not dealing with

phantom models, so that  $1 + w > 0$ . Second, we note that  $dp/d\rho = c_s^2$ , and we will assume further that  $c_s^2 > 0$ , to avoid instabilities in perturbation growth. These constraints are satisfied by most barotropic fluids of interest, although it is also possible to construct models which violate both assumptions (see, e.g., Ref. [14]). With these assumptions, equation (7) gives the limit

$$w' < 3w(1 + w). \quad (8)$$

This limit is shown in Fig. 1, where we have used the same scale as Ref. [17] for easy comparison. Note that this is

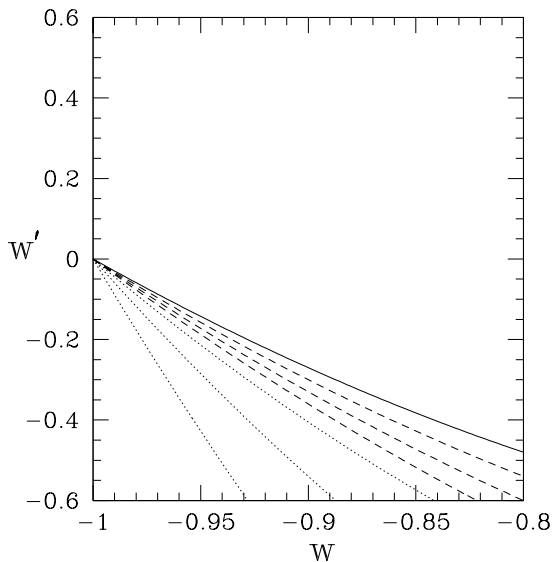


FIG. 1: Solid curve gives the upper bound on  $w'$  as a function of  $w$  for non-phantom barotropic models with positive squared sound speed. Dotted curves give  $w'$  as a function of  $w$  for Chaplygin gas dark energy with (top to bottom)  $\alpha = 0.5$ ,  $\alpha = 1$ ,  $\alpha = 2$ , while  $\alpha = 0$  lies on the solid curve. Dashed curves give  $w'$  as a function of  $w$  for the wet dark fluid model with (top to bottom)  $w_* = 0.1$ ,  $w_* = 0.2$ ,  $w_* = 0.3$ .

the exact opposite of the limit derived in Ref. [17] for “freezing” quintessence models:

$$w' > 3w(1 + w). \quad (9)$$

Thus, barotropic fluids and freezing quintessence models occupy non-overlapping regions in the  $w - w'$  plane. The bound in equation (8) is saturated when  $c_s^2 = dp/d\rho = 0$ , which corresponds to the case  $p = \text{constant}$ . In this case, we have  $w' = 3w(1 + w)$ . Models of this kind are particularly interesting, since they correspond to a barotropic fluid that behaves exactly like a mixture of dark matter (dust) and a cosmological constant. Such models can be constructed in the context of either the generalized Chaplygin gas [18] or  $k$ -essence [19].

Now consider several illustrative special cases. For the generalized Chaplygin gas, the equation of state is given by

$$p = -\frac{A}{\rho^\alpha}, \quad (10)$$

where  $A$  and  $\alpha$  are constants. (The Chaplygin gas corresponds to the special case  $\alpha = 1$ ). Then it is straightforward to use equation (7) to derive

$$w' = 3(1 + \alpha)w(1 + w). \quad (11)$$

This behavior is displayed in Fig. 1 for several values of  $\alpha$ . The  $\alpha = 0$  case saturates the upper bound on  $w'$ , as it corresponds to the previously-noted  $p = \text{constant}$  model, while the original Chaplygin gas model ( $\alpha = 1$ ) gives  $w' = 6w(1 + w)$ .

Another barotropic model is the wet dark fluid model of Ref. [16], with equation of state

$$p = w_*(\rho - \rho_*), \quad (12)$$

where  $w_*$  and  $\rho_*$  are constants. Again, it is straightforward to use equation (7) to derive the result

$$w' = -3(1 + w)(w_* - w), \quad (13)$$

which is displayed in Fig. 1 for several values of  $w_*$ .

While we have assumed that the fluid characterized by  $w'$  and  $w$  acts strictly as dark energy, all of the results derived here can also be applied to unified dark energy models, in which the barotropic fluid serves as both dark matter and dark energy (indeed, this is one of the main motivations for the Chaplygin gas model and its variants). However, in the case of unified dark energy,  $w$  and  $w'$  refer to the entire fluid, not just to the dark energy component.

### III. QUINTESSENCE

The equation of motion for the quintessence field  $\phi$  is

$$\ddot{\phi} + 3H\dot{\phi} + \frac{dV}{d\phi} = 0, \quad (14)$$

where the Hubble parameter  $H$  is

$$H = \frac{\dot{a}}{a} = \left(\frac{\rho}{3}\right)^{1/2}, \quad (15)$$

and  $\rho$  is the total density. (We assume an  $\Omega = 1$  universe and take  $8\pi G = 1$  throughout). Since we are interested in the late-time evolution of the dark energy, we assume that  $\rho = \rho_M + \rho_\phi$ , where  $\rho_M$  is the density of the matter, scaling as  $\rho_M \propto a^{-3}$ , and  $\rho_\phi$  is the scalar field energy density, given by

$$\rho_\phi = \frac{\dot{\phi}^2}{2} + V(\phi). \quad (16)$$

The pressure of the scalar field is

$$p_\phi = \frac{\dot{\phi}^2}{2} - V(\phi). \quad (17)$$

Caldwell and Linder [17] examined models in which  $\phi$  evolves toward the state  $V(\phi) = 0$ . They distinguished

two cases: “thawing” models, in which  $w \approx -1$  initially, but  $w$  increases as  $\phi$  rolls down the potential, and “freezing” models, in which  $w > -1$  initially, but  $w$  approaches  $-1$  as the field rolls down the potential. The bounds derived in Ref. [17] are based on a combination of plausibility arguments and numerical simulations. For the “thawing” models, these limits are

$$1 + w < w' < 3(1 + w), \quad (18)$$

while for the “freezing” models,

$$3w(1 + w) < w' < 0.2w(1 + w). \quad (19)$$

As noted in the previous section, the allowed region for barotropic fluids in the  $w - w'$  plane lies adjacent to the lower bound on  $w'$  for quintessence models proposed in Ref. [17]. Therefore, it is the lower bound in equation (19) which is of greatest interest here.

We first generalize the Caldwell-Linder lower bound to a wider range of potentials. Consider a scalar field evolving in an arbitrary monotonic potential  $V(\phi)$ , not necessarily asymptotically zero. We will take  $V'(\phi) < 0$ , but of course the argument is identical in the opposite case. Now, following Steinhardt et al. [6], we note that the equation of motion for  $\phi$  can be rewritten as

$$-\frac{V'}{V} = \sqrt{\frac{3(1+w)}{\Omega_\phi}} \left[ 1 + \frac{X'}{6} \right], \quad (20)$$

where  $X$  is defined as

$$X = \ln \left( \frac{1+w}{1-w} \right), \quad (21)$$

and  $X'$  is the derivative of  $X$  with respect to  $\ln(a)$ , so that  $X'$  and  $w'$  are related via

$$X' = \frac{2w'}{(1-w)(1+w)}. \quad (22)$$

Now we note that for a scalar field rolling downhill in a monotonically decreasing potential, the left-hand side of equation (20) is always positive. This, in turn, implies that  $1 + X'/6 > 0$ , which translates into the following bound on  $w'$ :

$$w' > -3(1-w)(1+w). \quad (23)$$

While not as tight as the Caldwell-Linder bound, equation (23) applies to a more general class of models; it assumes nothing about tracking behavior or “freezing” of the scalar field, nor is it confined to potentials for which  $V(\phi) \rightarrow 0$  asymptotically. This bound is saturated by a scalar field rolling on the constant potential  $V = V_0$ . For this case,  $w$  evolves from  $w \approx +1$  to  $w \approx -1$ , with  $w' = -3(1-w)(1+w)$  [20]. The bound in equation (23), along with the lower bound on  $w'$  from Ref. [17], are shown in Fig. 2.

We can tighten this bound considerably for the case of “tracker” models, i.e., models for which  $w$  is initially

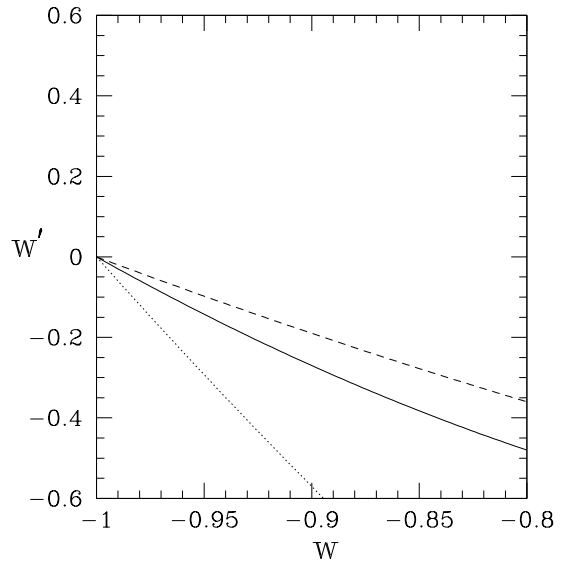


FIG. 2: Solid curve gives the lower bound on  $w'$  as a function of  $w$  for “freezing” quintessence models from Ref. [17]. Dotted curve gives our lower bound on  $w'$  as a function of  $w$  for quintessence models with an arbitrary monotonic potential (equation 23). Dashed curve gives our lower bound on  $w'$  as a function of  $w$  for tracker quintessence models (equation 31).

constant when  $\rho_\phi \ll \rho_M$ , but which evolve toward  $w = -1$  when  $\rho_\phi \approx \rho_M$ . Again, following Ref. [6], we define  $\Gamma$  to be given by

$$\Gamma \equiv \frac{V''V}{V'^2}. \quad (24)$$

If  $w_B$  is the equation of state parameter for the background fluid, then tracking behavior with  $w < w_B$  occurs when  $\Gamma$  is roughly constant with  $\Gamma > 1$  [6]. Note that  $\Gamma$  is exactly constant for power law and exponential potentials. In particular, for the potential  $V \propto \phi^{-\alpha}$ , we have  $\Gamma = 1 + 1/\alpha$ . Taking the derivative of equation (20) with respect to  $\phi$  gives

$$\begin{aligned} \Gamma = 1 - \frac{2X''}{(1+w)(6+X')^2} - \frac{1-w}{2(1+w)} \frac{X'}{6+X'} \\ + \frac{3(w_B-w)}{1+w} \frac{1-\Omega_\phi}{6+X'}. \end{aligned} \quad (25)$$

Note that this equation differs from the corresponding equation in Ref. [6] because we do not take the limit  $\Omega_\phi \rightarrow 0$ ; all of the interesting evolution occurs when  $\rho_\phi$  becomes significant compared to  $\rho_M$ . It does however, agree with the expression previously derived in Ref. [21], and in the limit where  $\Omega_\phi \rightarrow 0$ , equation (25) reduces to the corresponding equation in Ref. [6].

When the tracker solution is reached, and the background fluid dominates,  $w$  is a constant. We will be interested in the late-time evolution of the quintessence field, so we assume that the background fluid is cold dark

matter, with  $w_B = 0$ . Then for the tracker solution, taking  $X'' = X' = 0$  and  $\Omega_\phi = 0$  in equation (25) gives

$$w = \frac{-2(\Gamma - 1)}{2(\Gamma - 1) + 1} \quad (26)$$

In this regime,  $\Omega_\phi$  increases with time; when  $\Omega_\phi$  is no longer negligible with respect to 1, the tracker solution no longer applies. At this point,  $w$  decreases, asymptotically approaching  $w = -1$ . (See Ref. [22] for a discussion of the evolution in this regime).

Since  $w' \leq 0$  for these tracker solutions, we have  $X' \leq 0$ . Initially,  $X' = 0$ , but as  $\Omega_\phi$  becomes nonnegligible,  $X'$  decreases. It reaches some minimum value,  $X'_{min}$ , but then increases back to a value near zero as  $\Omega_\phi \rightarrow 1$ . This behavior is illustrated in Fig. 3, in which we show the evolution for  $X'$  as a function of  $\Omega_\phi$  for several power-law potentials. The value of  $X'_{min}$  is the key to our

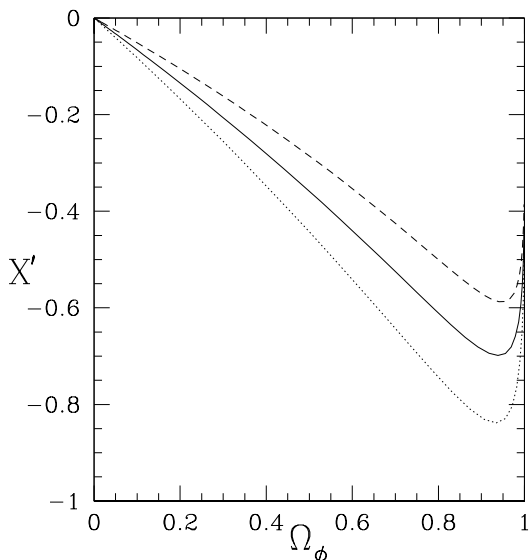


FIG. 3: The evolution of  $X'$  as a function of  $\Omega_\phi$  for the potential  $V(\phi) \propto \phi^{-\alpha}$  with  $\alpha = 2$  (dashed curve),  $\alpha = 1$  (solid curve) and  $\alpha = 0.2$  (dotted curve).

calculation, since it gives a lower bound on  $w'$  through equation (22).

To find this minimum value for  $X'$ , we simply take  $X'' = 0$  in equation (25), where we assume also that  $w_B = 0$  and that  $\Gamma$  is nearly constant. This gives

$$X'_{min} = -6 \frac{(1 - \Omega_\phi)w + 2(\Gamma - 1)(1 + w)}{(1 - w) + 2(\Gamma - 1)(1 + w)}. \quad (27)$$

On the right-hand side of this equation,  $w$ ,  $\Omega_\phi$ , and  $\Gamma$  are to be evaluated at the point at which  $X' = X'_{min}$ . In general  $\Omega_\phi$  and  $w$  evolve in a complex fashion (see, e.g., Ref. [22]), so equation (27) does not have a simple solution. However, since we seek a lower bound on  $X'$ , it is sufficient to use equation (27) to find a lower bound

on  $X'_{min}$ . We first note that  $\Omega_\phi < 1$ ; applying this limit (with  $w < 0$ ) to equation (27) yields

$$X'_{min} > -6 \frac{2(\Gamma - 1)(1 + w)}{(1 - w) + 2(\Gamma - 1)(1 + w)}. \quad (28)$$

The right-hand side of equation (28) increases with decreasing  $w$ , so a lower bound on the right-hand side is achieved by assigning the maximum allowed value to  $w$ . In tracker models,  $w$  decreases from the initial value given by equation (26), so substituting the value for  $w$  given by equation (26) into equation (28) gives a lower bound on  $X'_{min}$ :

$$X'_{min} > -\frac{12(\Gamma - 1)}{6(\Gamma - 1) + 1}. \quad (29)$$

Taking  $X' > X'_{min}$ , and using equation (22) to convert from  $X'$  to  $w'$ , we obtain the limit

$$w' > -\frac{6(\Gamma - 1)}{6(\Gamma - 1) + 1}(1 - w)(1 + w). \quad (30)$$

This is obviously a model-dependent result, since it depends on the value of  $\Gamma$  for which tracking behavior is achieved. However, we can use it to derive a more general limit by noting that, since  $\Gamma > 1$ , we have  $6(\Gamma - 1)/[6(\Gamma - 1) + 1] < 1$ , giving

$$w' > -(1 - w)(1 + w). \quad (31)$$

Equation (31) gives a lower bound on  $w'$  for tracker models. This bound is shown in Fig. 2. This is clearly a very conservative limit; for example, it is obvious from Fig. 3 that the value of  $X'_{min}$  is often obtained for a value of  $\Omega_\phi$  larger than is consistent with observations. However, equation (31) does give a tighter bound than that derived in Ref. [17], further separating quintessence models from the barotropic fluid models discussed in the previous section.

#### IV. DISCUSSION

Our results illustrate the usefulness of the  $w - w'$  plane as a means for observationally distinguishing dark energy models. Non-phantom barotropic fluid models with positive squared sound speed and “tracker” quintessence models occupy disjoint regions in this plane. Even our less stringent general limit on quintessence models with monotonic potentials is inconsistent with a wide class of barotropic fluid models, as can be seen by comparing Figs. 1 and 2.

Supernova Ia measurements [23, 24] have narrowed the range of possible values for  $w$ ; in particular, they are consistent with  $w \approx -1$ . The value of  $w'$  is less well constrained (see, e.g., Ref. [24]). The results of Ref. [17] indicate that the resolution on a measurement of  $w'$  must be of order  $1 + w$  in order to distinguish “freezing” and

“thawing” quintessence models. We reach a similar conclusion with regard to barotropic fluids and quintessence models: observationally distinguishing between these two classes of models also requires that  $\sigma(w') \lesssim 1 + w$ .

Finally, we note that there is a relation between the  $w - w'$  parametrization of Ref. [17] and the “statefinder” pair introduced in Ref. [25]. The statefinders  $r$  and  $s$  are defined by

$$r = \frac{\ddot{a}}{aH^3}, \quad (32)$$

$$s = \frac{r - 1}{3(q - 1/2)}, \quad (33)$$

where  $q = -a\ddot{a}/\dot{a}^2$  is the deceleration parameter. Then  $r$  and  $s$  are related to  $w$  and  $w'$  via [25]

$$r = 1 + \frac{9}{2}\Omega_{DE}w(1+w) - \frac{3}{2}\Omega_{DE}w', \quad (34)$$

$$s = 1 + w - \frac{w'}{3w}, \quad (35)$$

where  $\Omega_{DE}$  is the fraction of the total energy density contributed by the dark energy. Note, however, that the mapping between  $w$ ,  $w'$  and  $r$ ,  $s$  is non-trivial because of the factor of  $\Omega_{DE}$  in equation (34). For non-constant  $w$ , the evolution of  $\Omega_{DE}$  depends in a complicated way on both  $a$  and  $w(a)$ . Hence, the statefinder parameters encode somewhat different information about the behavior of the dark energy than do  $w$  and  $w'$ . The statefinder parameters are more directly related to observable quantities, while the  $w - w'$  parametrization describes more directly the physical properties of the dark energy.

### Acknowledgments

I thank A. A. Sen, R. Caldwell, and E. Linder for helpful discussions. I am grateful to E. Babichev and C. Rubano for helpful comments on the manuscript. R.J.S. was supported in part by the Department of Energy (DE-FG05-85ER40226).

- 
- [1] V. Sahni, astro-ph/0403324.
  - [2] B. Ratra and P.J.E. Peebles, Phys. Rev. D **37**, 3406 (1988).
  - [3] M.S. Turner and M. White, Phys. Rev. D **56**, 4439 (1997).
  - [4] R.R. Caldwell, R. Dave, and P.J. Steinhardt, Phys. Rev. Lett. **80**, 1582 (1998).
  - [5] A.R. Liddle and R.J. Scherrer, Phys. Rev. D **59**, 023509 (1999).
  - [6] P.J. Steinhardt, L. Wang, and I. Zlatev, Phys. Rev. D **59**, 123504 (1999).
  - [7] A.Y. Kamenshchik, U. Moschella, and V. Pasquier, Phys. Lett. B **511**, 265 (2001).
  - [8] N. Bilic, G.B. Tupper, and R.D. Viollier, Phys. Lett. B **535**, 17 (2002).
  - [9] M.C. Bento, O. Bertolami, and A.A. Sen, Phys. Rev. D **66**, 043507 (2002).
  - [10] A. Dev, J.S. Alcaniz, and D. Jain, Phys. Rev. D **67**, 023515 (2003).
  - [11] V. Gorini, A. Kamenshchik and U. Moschella, Phys. Rev. D **67**, 063509 (2003).
  - [12] R. Bean and O. Dore, Phys. Rev. D **68**, 23515 (2003).
  - [13] T. Multamaki, M. Manera and E. Gaztañaga, Phys. Rev. D **69**, 023004 (2004).
  - [14] A.A. Sen and R.J. Scherrer, Phys. Rev. D **72**, 063511 (2005).
  - [15] S. Capozziello et al., JCAP **04**, 005 (2005).
  - [16] E. Babichev, V. Dokuchaev, and Yu. Eroshenko, Class. Quant. Grav. **22**, 143 (2005); R. Holman and S. Naidu, astro-ph/0408102.
  - [17] R.R. Caldwell and E.V. Linder, Phys. Rev. Lett. **95**, 141301 (2005).
  - [18] P.P. Avelino, L.M.G. Beca, J.P.M. de Carvalho, and C.J.A.P. Martins, JCAP **09**, 002 (2003).
  - [19] R.J. Scherrer, Phys. Rev. Lett. **93**, 011301 (2004).
  - [20] E.V. Linder, Astropart. Phys. **24**, 391 (2005).
  - [21] C. Rubano, et al., Phys. Rev. D **69**, 103510 (2004).
  - [22] C.R. Watson and R.J. Scherrer, Phys. Rev. D **68**, 123524 (2003).
  - [23] R.A. Knop, et al., Astrophys. J. **598**, 102 (2003).
  - [24] A.G. Riess, et al., Astrophys. J. **607**, 665 (2004).
  - [25] V. Sahni, T.D. Saini, A.A. Starobinsky, and U. Alam, JETP Lett. **77**, 201 (2003); U. Alam, V. Sahni, T.D. Saini, and A.A. Starobinsky, MNRAS **344**, 1057 (2003).